



Lunar pure anorthosite as a spectral analog for Mercury

DAVID T. BLEWETT^{1*}, B. RAY HAWKE² AND PAUL G. LUCEY²

¹NovaSol, 1100 Alakea Plaza, 23rd Floor, Honolulu, Hawaii 96813, USA

²Hawaii Institute of Geophysics and Planetology, University of Hawaii, Honolulu, Hawaii 96822, USA

*Correspondence author's e-mail address: dave.blewett@nova-sol.com

(Received 2002 March 9; accepted in revised form 2002 June 7)

(Presented at the Workshop on Mercury, The Field Museum, Chicago, Illinois, 2001 October 4–5)

Abstract—Plans are underway for spacecraft missions to the planet Mercury beginning in the latter part of this decade (NASA's MESSENGER (MERcury, Surface, Space ENvironment, GEOchemistry, Ranging) and ESA's BepiColombo). Mercury is an airless body whose surface is apparently very low in ferrous iron. Much of the mercurian surface material is expected to be optically mature, a state produced by the "space weathering" process from direct exposure to the space environment. If appropriate analog terrains can be identified on the Moon, then study of their reflectance spectra and composition will improve our understanding of space weathering of low-Fe surfaces and aid in the interpretation of data returned from Mercury by the spacecraft.

We have conducted a search for areas of the lunar surface that are optically mature and have very low ferrous iron content using Clementine ultraviolet–visible (UV-vis) image products. Several regions with these properties have been identified on the farside. These areas, representing mature pure anorthosites (>90% plagioclase feldspar), are of interest because only relatively immature pure anorthosites have previously been studied with Earth-based spectrometry. A comparison of Mercury with the lunar analogs reveals similarities in spectral characteristics, and there are hints that the mercurian surface may be even lower in FeO content than the lunar pure anorthosites.

We also investigate the potential for use of spectral features other than the commonly studied "1 μm " mafic mineral absorption band as tools for compositional assessment when spacecraft spectral measurements of Mercury become available. Most low-Fe minerals plausibly present on Mercury lack absorption bands, but plagioclase possesses an iron impurity absorption at 1.25 μm . Detection of this diagnostic band may be possible in fresh crater deposits.

INTRODUCTION

The Moon and Mercury are the two smallest planetary bodies in the inner solar system. Despite a first order similarity in surface morphology, the presence of a large dense core in Mercury indicates that the two objects must have important fundamental differences in their formation and geologic evolution. In contrast to the extensive knowledge of the Moon gained through Earth-based remote sensing, spacecraft exploration and sample return, little is known about the surface composition of Mercury.

Remote sensing measurements at a variety of wavelengths indicate that the surface of Mercury must be low in iron and titanium, with FeO + TiO₂ less than ~6 wt% (e.g., Vilas, 1988, and references therein; Sprague *et al.*, 1994; Jeanloz *et al.*, 1995). Reflectance spectrometry from Earth-based telescopes has discovered small areas of the nearside of the Moon that lack the otherwise ubiquitous ferrous iron absorption band near

1 μm (Spudis *et al.*, 1984, 1989; Pieters, 1986, 1993; Hawke *et al.*, 1991, 1993a,b). These areas thus must be extremely low in FeO, <2–3 wt%, and are believed to be composed of >90% plagioclase feldspar. According to the lunar highland rock classification scheme of Stöffler *et al.* (1980), such a lithology is referred to as pure anorthosite. Global imaging of the Moon by the *Clementine* spacecraft (Nozette *et al.*, 1994; Robinson and McEwen, 1997), along with a method for the determination of FeO abundance from the *Clementine* ultraviolet–visible (UV-vis) camera multispectral measurements (Lucey *et al.*, 1995, 1998, 2000a; Blewett *et al.*, 1997a) has led to the identification of large regions of the lunar farside that are low in FeO content. In addition, an analysis by Tompkins and Pieters (1999) using *Clementine* UV-vis spectral parameters indicates that a number of highland crater central peaks may be composed of pure anorthosite. The present work extends a previous study by Blewett *et al.* (1997b), which compared spectra of Mercury to those of lunar anorthosites.

The lunar pure anorthosites discovered with Earth-based telescopes (limited to examining the nearside) are areas such as small fresh craters, massifs and crater central peaks. These bright features contribute greater amounts of reflected light to the spectrometer, yielding higher quality spectra, and provide information on the properties of material least affected by space weathering. "Space weathering" is a term for the processes affecting the surface material of an airless solar system object. Direct exposure to fluxes of micrometeorites, the solar wind and cosmic rays produces physical and chemical changes in the surface material. Of particular importance is the production of vapor-phase deposits of submicroscopic metallic iron (SMFe, also termed nanophase iron) on soil grains during space weathering. The accumulation of SMFe with continued surface exposure is largely responsible for the optical changes that occur as a soil matures (see Pieters *et al.* (2000) for a review of the current state of knowledge concerning space weathering). The areas of pure anorthosite identified with telescopic spectra have a low degree of optical maturity (*i.e.*, they have relatively little accumulation of space-weathered material). This is a result of young age (as in the case of small fresh craters) or because down-slope movement on steep topography (massifs and crater central peaks) continually exposes fresh material.

Pure anorthosites are often found in association with basin rings, and give important clues to lunar stratigraphy and crustal origin (Spudis *et al.*, 1984; Pieters, 1986; Hawke *et al.*, 1993b, 2002; Peterson *et al.*, 2001). Figure 1 shows two of the highest quality telescopic near-infrared reflectance spectra of pure anorthosites. The spectra display an increase in reflectance with increasing wavelength (red spectral slope), and no absorption features. Specifically lacking is an absorption feature near $1\ \mu\text{m}$ caused by ferrous iron in silicate minerals or glasses. Absence of this absorption band indicates that iron-bearing pyroxenes or olivines can only be present at levels below $\sim 5\%$, and hence the locations for which the spectra were obtained are classified as pure anorthosite. Figure 1 also shows Clementine UV-vis spectra for approximately the same locations as the telescopic near-infrared spectra.

If mature lunar anorthosites can be identified, they may furnish a better spectral analog for Mercury. No Earth-based telescopic spectra of fully mature lunar pure anorthosites exist.

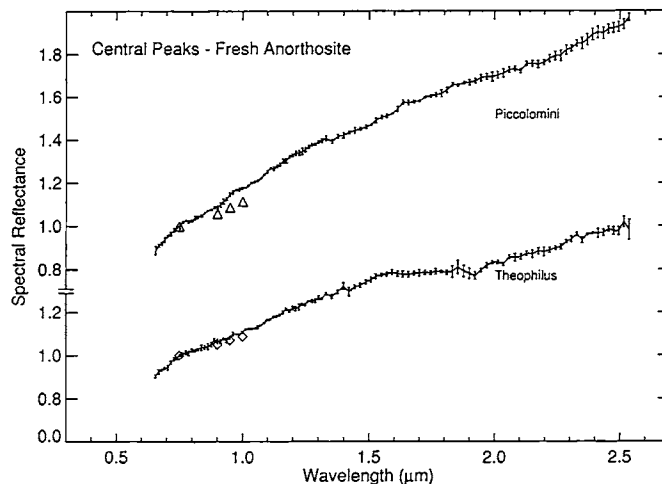


FIG. 1. Near-infrared reflectance spectra of pure anorthositic central peaks, with Clementine UV-vis spectra (triangles, diamonds) of approximately the same area. All spectra have been scaled to 1.0 at $0.75\ \mu\text{m}$. Piccolomini is located at $\sim 29.7^\circ\ \text{S}$, $32.2^\circ\ \text{E}$. Theophilus is located at $\sim 11.4^\circ\ \text{S}$, $26.4^\circ\ \text{E}$. These spectra were collected with the Planetary Geosciences IRCVF spectrometer mounted on the University of Hawaii 2.2 m telescope on Mauna Kea (see Pieters, 1986).

Disc-integrated spectra of Mercury should be dominated by mature material because fresh crater deposits make up only a small proportion of the surface area. In addition, the space environment at Mercury may be such as to promote greater rates and states of optical maturity than the Moon (Cintala, 1992).

SEARCHING FOR MATURE LUNAR ANORTHOSITES

In order to locate areas of mature lunar anorthosite, we conducted a search using FeO and optical maturity maps prepared with the algorithms of Lucey *et al.* (2000a,b). The maps were constructed from 1 km/pixel Clementine UV-vis mosaics (Eliason *et al.*, 1999; Isbell *et al.*, 1999; Robinson *et al.*, 1999). The Lucey method for mapping FeO content relies on 750 nm reflectance and 950/750 nm ratio images to measure the spectral effects of ferrous iron in lunar mafic minerals. The technique controls for the competing optical influence of the SMFe that is produced as space weathering proceeds.

TABLE 1. Data on regions of mature pure anorthosite identified in Clementine images.

Region	Latitude/longitude	Area (km ²)	Average FeO (wt%)	Average OMAT value	Geologic unit
1	29.1° N, 224.6° E	2113	3.1 ± 0.5	0.157 ± 0.010	Ip/INt
2	4.0° N, 231.7° E	1622	3.3 ± 0.6	0.138 ± 0.010	Nhb/Iohs
3	29.8° N, 187.9° E	2151	3.0 ± 0.7	0.145 ± 0.010	NpNt
4	27.0° N, 169.8° E	3834	2.8 ± 0.7	0.146 ± 0.012	NpNt

Abbreviations: OMAT = optical maturity parameter; Ip = Imbrian plains material; INt = Imbrian/Nectarian undivided terra material (Scott *et al.*, 1977); Nhb = Nectarian Hertzprung basin material; Iohs = Imbrian secondary crater facies (Scott *et al.*, 1977); NpNt = Nectarian irregular terra (Stuart-Alexander, 1978).

Evidence that the Lucey spectral method reliably determines FeO abundance at locations distant from the sample-return sites with which it was calibrated is provided by Earth-based spectra and Lunar Prospector geochemical measurements. First, areas known to be composed of pure anorthosite from their telescopic near-infrared spectral characteristics are indeed found to have very low iron values in Clementine FeO maps (Hawke *et al.*, 2002). Second, Prospector neutron spectrometer measurements of iron abundance and independent measurements of iron by the Prospector gamma-ray spectrometer both show very good correlations with Clementine FeO maps (Elphic *et al.*, 1998, 2000; Lawrence *et al.*, 2002).

The optical maturity parameter (OMAT) is the complement to the spectral iron parameter (Lucey *et al.*, 2000b; Grier *et al.*, 2001). OMAT maps provide a measure of the maturity state of the surface that is largely independent of bulk composition. Figure 2 presents FeO and OMAT images of the lunar western hemisphere. The FeO map shows very little correlation with the freshness of the surface (bright craters and rays are generally not apparent). In the OMAT image, variations controlled by composition are largely absent. Large tracts of the northern farside possess very low iron abundances.

In order to find optically mature areas with low iron abundance, FeO and OMAT images were simultaneously displayed. We sought areas with very low values in both images (a low OMAT value corresponds to a high degree of maturity). Slopes that might produce erroneous values because of uncorrected topographical control of surface albedo were avoided. In the initial survey, four candidate regions were located, each containing from ~1600 to 3800 pixels (each pixel covers ~1 km²). The average FeO of these areas, all of which are on the farside, ranges from 2.8 to 3.1 wt% (Table 1). They are located in plains or terra units of Imbrian or Nectarian age (Stuart-Alexander, 1978; Scott *et al.*, 1977).

Figure 3 shows the average UV-vis spectra of the four areas, along with the two immature anorthosites from Fig. 1 for comparison. The mature anorthosite regions are darker and have steeper spectral slopes than the fresh anorthosites. A closer view of one area is presented in Fig. 4, which shows a 500 × 500 km view of 1 km resolution data. Fresh material (bright in the OMAT image) is present in small impact craters and ray material crossing the image. The area outlined in white in Fig. 4 has both very low iron and very low OMAT values (area 2 in Table 1).

Moving to a 100 m/pixel-resolution view of a portion of area 2, Fig. 5 reveals uniformly low FeO and little contamination from rays originating beyond the image boundaries. Much of the surface in this region has extremely low FeO content and is quite mature. An average spectrum of a 3 × 3 pixel box near the center of the image was extracted (spectrum "2a") and is plotted in Fig. 6. This location has 1.4 wt% FeO and OMAT equal to 0.125. Figure 6 also shows the average area 2 spectrum from Fig. 3 for comparison. Overall, area 2 is slightly less mature (higher OMAT) than the small sub-area from which

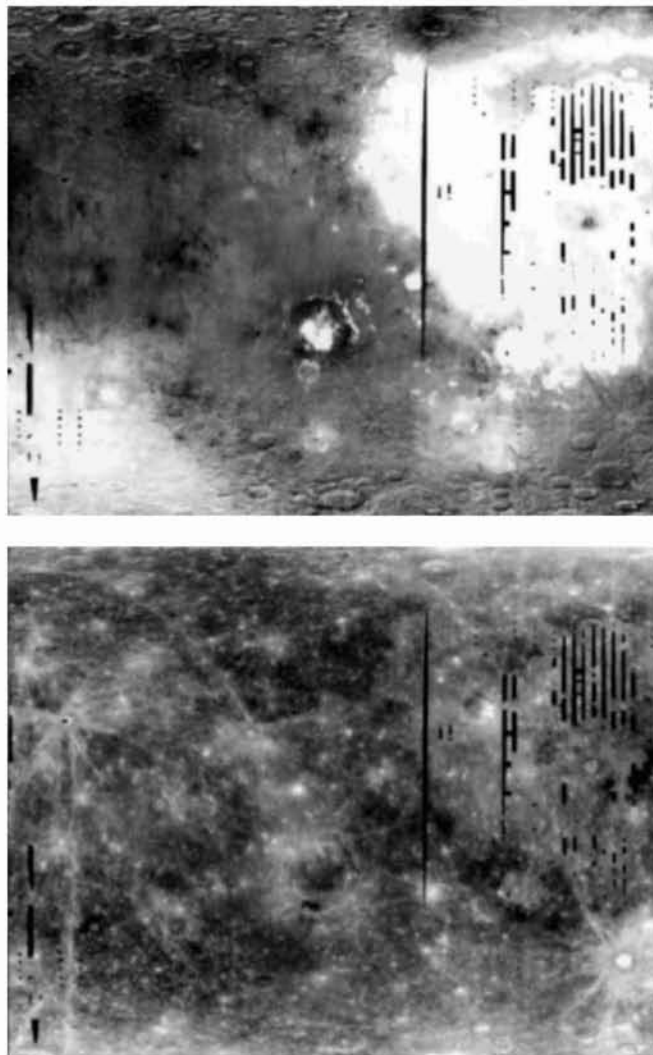


FIG. 2. Compositional and optical maturity images of the Moon's western hemisphere. (Top) Clementine FeO image. Brighter tones indicate a higher abundance of iron in the surface. (Bottom) Optical maturity image. Brighter tones indicate a higher OMAT parameter value, equivalent to a lower degree of optical maturity (*i.e.*, fresher = brighter, more mature = darker). Both images are simple cylindrical projections with north toward the top and east toward the right. The original spatial resolution of these images was 1 km/pixel. Center latitude = 0°, center longitude = 270° E. The latitude range is +70° to -70°, the longitude range is 180 to 360° E. The nearside maria are the high-FeO areas on the right side of the FeO image; the South Pole-Aitken basin is the moderate-to-high FeO area in the lower left corner. Tycho crater, near the lower right edge, is prominent in the OMAT image.

spectrum 2a was extracted (Fig. 6, top). Thus the area 2 spectrum has slightly higher albedo. In the plot showing spectra normalized at 0.75 μm (Fig. 6, bottom), the greater maturity of the 100 m/pixel spectrum causes it to have a slightly steeper (redder) spectral slope longwards of 0.75 μm .

An examination of 100 m/pixel images of the other three areas listed in Table 1 found mature, low FeO surfaces with spectra that are nearly identical to those shown in Fig. 6. The

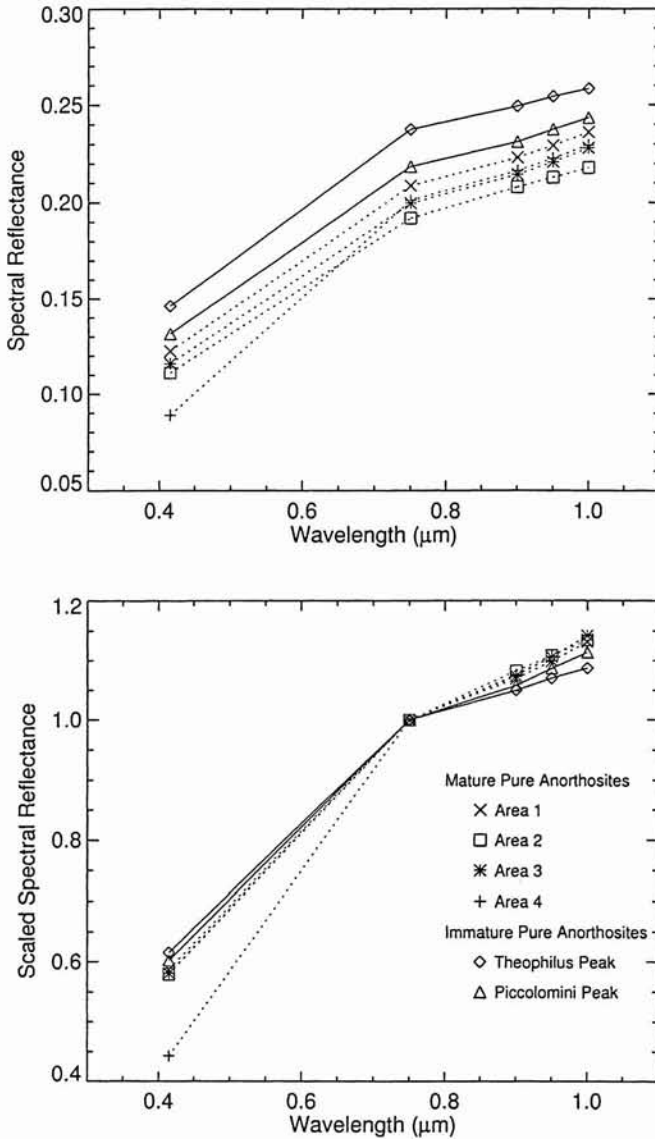


FIG. 3. Average Clementine UV-vis spectra of four farside areas of pure anorthosite and the two nearside pure anorthosite central peaks from Fig. 1. All spectra are essentially flat from 0.75 to 1.0 μm , indicating a lack of a 1 μm mafic mineral absorption band at this spectral resolution. Immature spectra are have higher overall reflectance and have slopes in the 0.75 to 1.0 μm range that are less steep than spectra of mature areas. (Top) Reflectance spectra. (Bottom) Spectra scaled to 1.0 at 0.75 μm to emphasize differences in slope.

identification of these areas establishes the existence of lunar mature pure anorthosites and provides the first information on their spectral properties. This mature pure anorthosite material is a plausible analog for much of the surface of Mercury.

COMPARISON TO MERCURY

The spectrum of the lunar mature pure anorthosite identified in the previous section may be compared to available spectra of Mercury. Mercury is a very difficult target for Earth-based

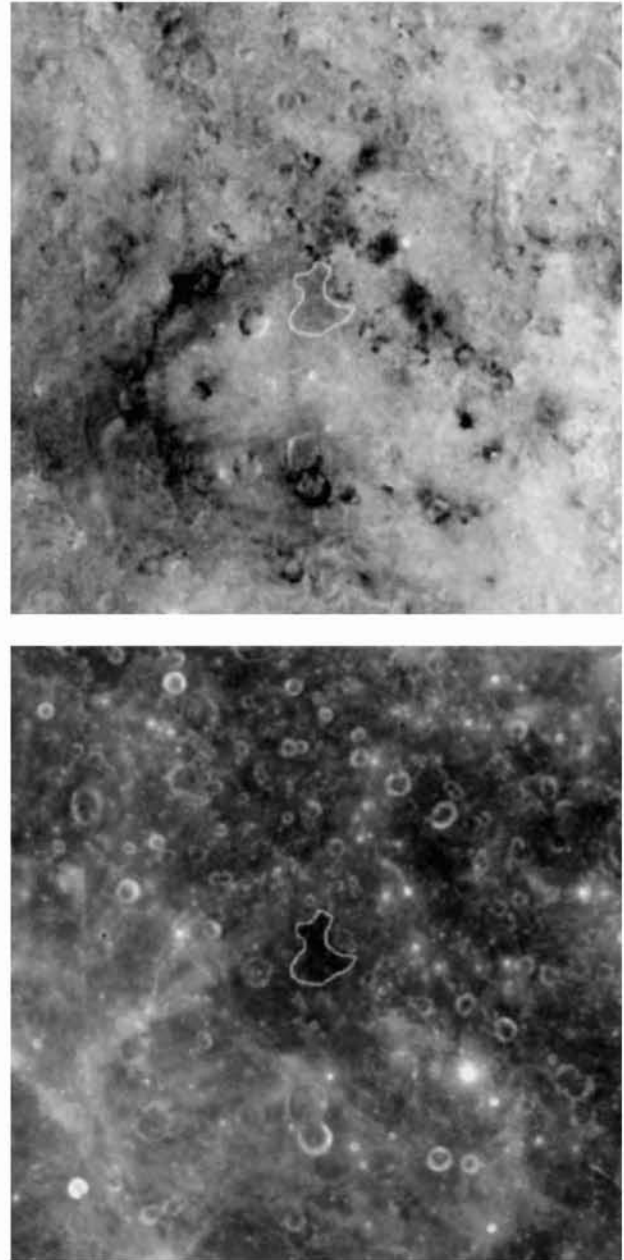


FIG. 4. Clementine compositional and optical maturity images of a region of mature pure anorthosite. (Top) FeO image stretched 0 to 7 wt% FeO. (Bottom) Optical maturity image stretched 0.095 to 0.294. The area shown is $\sim 500 \times 500$ km. Simple cylindrical projections centered at $\sim 4.0^\circ$ N, 231.7° E. The original spatial resolution of these images was 1 km/pixel. The region outlined in white is area 2 of Table 1. The outline was drawn to select material with low FeO and low OMAT. The average UV-vis spectrum of this area is plotted in Fig. 3 (squares). A close-up of an area within the outline is shown in Fig. 5.

observation because its angular separation from the Sun is never very great. The planet must therefore be observed near sunrise or sunset when the path through Earth's atmosphere is long (high airmass). These conditions make spectral calibration and removal of telluric features problematic. Vilas' (1988) review

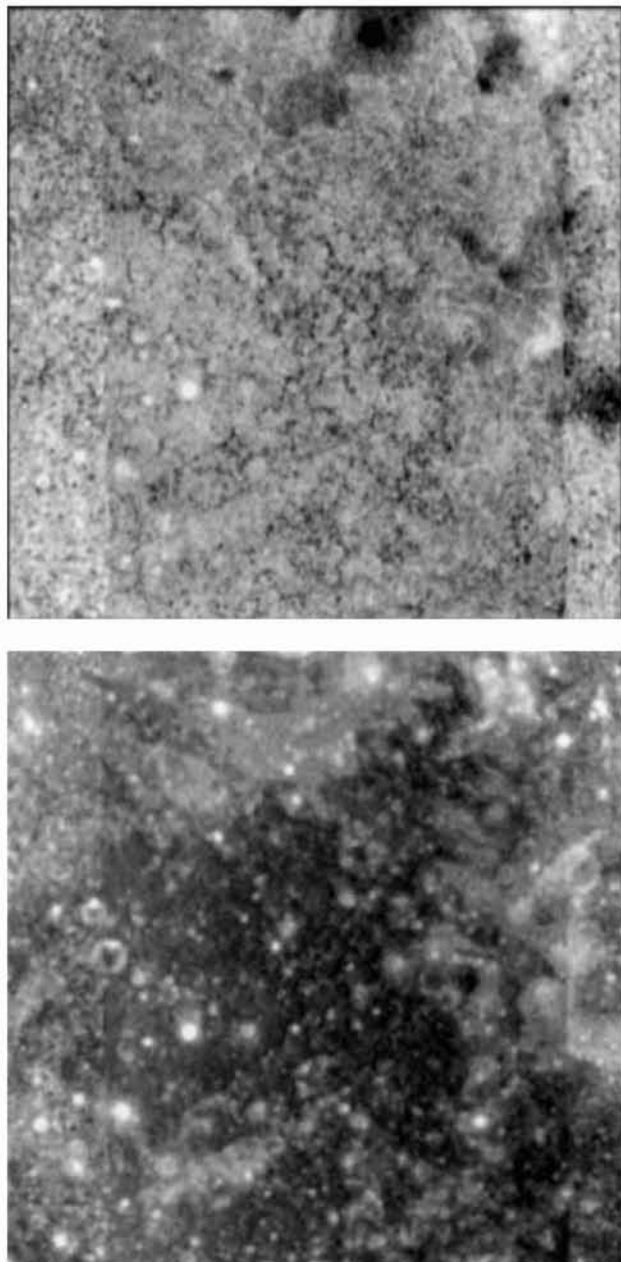


FIG. 5. Clementine compositional and optical maturity images of a region of mature pure anorthosite. (Top) FeO image stretched 0 to 6 wt% FeO. (Bottom) Optical maturity image stretched 0.10 to 0.21. The area shown is $\sim 50 \times 50$ km and lies mostly within the outlined region in Fig. 4. Simple cylindrical projections centered near 4.0° N, 231.7° E. The original spatial resolution of these images was 100 m/pixel.

of mercurian spectra considers one of the best-corrected Earth-based spectra of Mercury to be that collected in 1974 October (see also Blewett *et al.*, 1997b). Figure 7a is a plot of the October 1974 Mercury spectrum with the Clementine 100 m/pixel average UV-vis spectrum from Fig. 6. Figure 7b shows another extended-visible wavelength range spectrum of Mercury, the charge-coupled device (CCD) spectrum from 1984 November (Vilas, 1985). From Fig. 7a,b, it can be seen that the lunar

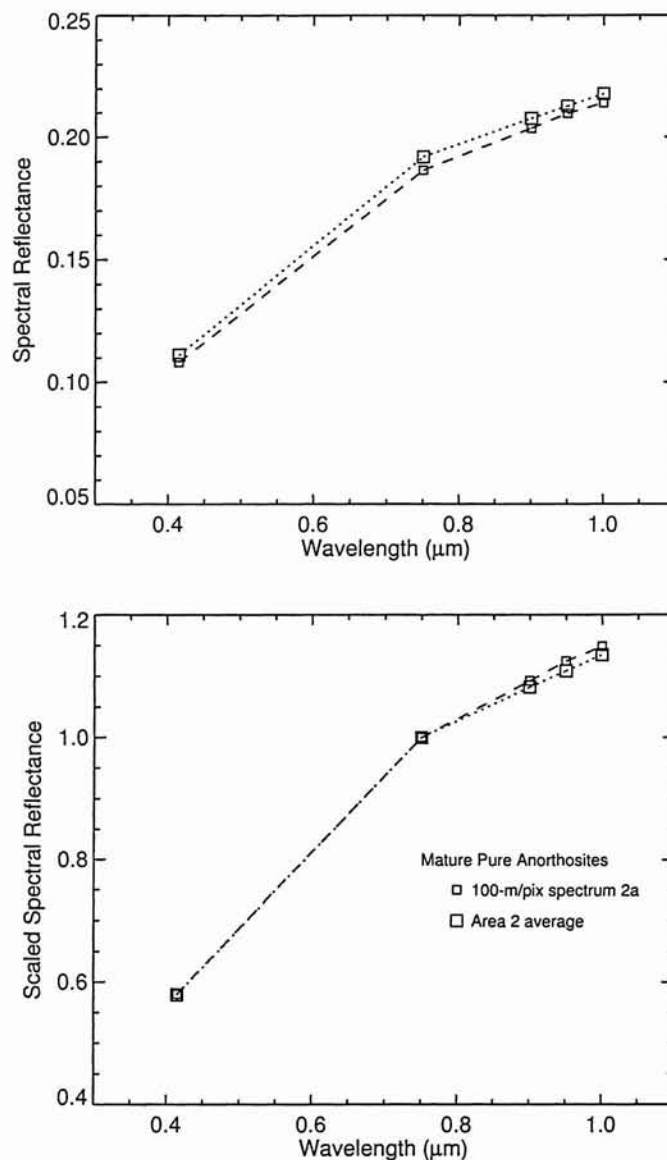


FIG. 6. Clementine UV-vis spectrum of a 3×3 pixel region near the center of Fig. 5 ("spectrum 2a", small squares with dashed line). This small area has an average FeO of 1.4 wt% and an average OMAT of 0.125. Shown for comparison is the spectrum of area 2 from Fig. 3 (large squares, dotted line). The material in locations such as this may be a good analog for Mercury. (Top) Reflectance spectra. (Bottom) Spectra scaled to 1.0 at $0.75 \mu\text{m}$ to emphasize differences in slope.

mature pure anorthosite and Mercury have very similar spectral slopes in the region ~ 0.40 to $0.75 \mu\text{m}$. The slopes longward of $0.75 \mu\text{m}$ are also similar, although the Mercury spectra appear to be somewhat redder (steeper). This is also the case for high-quality mercurian extended-visible spectra recently obtained by Warell (2002, unpubl. data) with the Swedish Vacuum Solar Telescope and the Nordic Optical Telescope.

Figure 7c presents the near-infrared circular variable filter spectrometer (IRCVF) spectrum of Mercury obtained on 1976 April 21 by McCord and Clark (1979). This spectrum has less overlap in wavelength range with the Clementine UV-vis data.

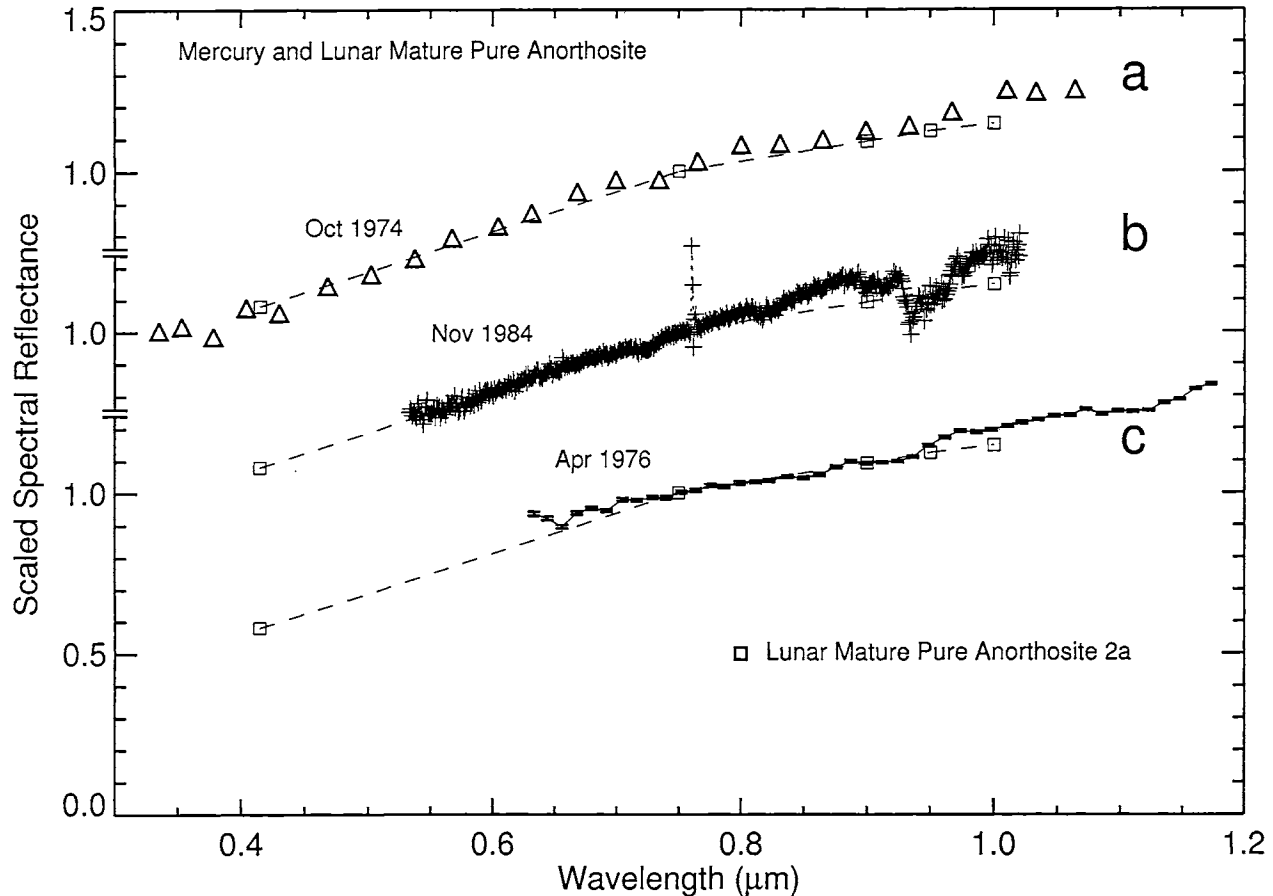


FIG. 7. Spectra of Mercury compared to a lunar mature pure anorthosite. The Clementine UV-vis 100 m/pixel average spectrum 2a from Fig. 6 is plotted with small squares. (a) The Mercury filter photometer spectrum from 1974 October (see Vilas, 1988) is plotted with triangles. (b) The Mercury CCD spectrum from 1984 November (Vilas, 1985, 1988) is plotted with +. Changing atmospheric conditions between the time of the Mercury and standard star observations led to the uncorrected water absorptions (most prominently near $0.9 \mu\text{m}$) in the 1984 Mercury spectrum. (c) The Mercury IRCVF spectrum from 1976 April 21 (McCord and Clark, 1979) is plotted with error bars. Only part of the IRCVF spectrum is shown; the full spectrum extends to $\sim 2.5 \mu\text{m}$. The spectra have been offset for clarity and are scaled to 1.0 at $0.75 \mu\text{m}$.

Here also the mercurian and lunar spectra have comparable slopes in the visible, but Mercury is slightly steeper in the near-infrared. The Clementine near-infrared camera collected lunar images in the wavelength range ~ 1.1 to $2.7 \mu\text{m}$. When calibration of the Clementine near-infrared dataset is completed, a more comprehensive comparison between the lunar pure anorthosites and the McCord and Clark spectrum of Mercury may be accomplished.

Therefore it can be concluded that reflectance spectra of Mercury and lunar mature pure anorthosites have important similarities. Both lack mineralogic absorption features and have very similar red slopes in the visible. At wavelengths greater than $\sim 0.75 \mu\text{m}$, Mercury may have a slightly steeper spectral slope. Lucey (2002) modeled a fresh lunar anorthosite spectrum and found that mixtures of anorthite with small amounts (1–4%) of iron-rich pyroxene could produce fits within the uncertainty of the data. The " $1 \mu\text{m}$ " ferrous absorption feature caused by the small pyroxene component would be expected to lower the reflectance in the near-infrared. Thus

the steeper spectral slope of the mercurian spectra could be explained by a pure anorthositic surface that is exceedingly low in ferrous iron, with amounts even less than the lunar pure anorthosites. The redness of the mercurian spectra does require the presence of some SMFe produced by space weathering, but this iron could be derived from meteoritic sources rather than from the mercurian country rock (Noble and Pieters, 2001). There are several uncertainties bearing on the conclusion that Mercury spectra are steeper at longer wavelengths, including atmospheric correction of the Mercury spectra, the possible effects of phase reddening, and the exact type of reflectance quantity (*e.g.*, Hapke, 1981, 1993) being compared. Apart from these uncertainties, further theoretical work using the model of Hapke (2001) could help to elucidate the slope difference between the mercurian and lunar analog spectra.

The lunar mature pure anorthosites are an excellent starting place for studying the composition of Mercury and the types of spectral variations to be expected there. The telescopic lunar spectra, the Clementine UV-vis and near-infrared datasets, and

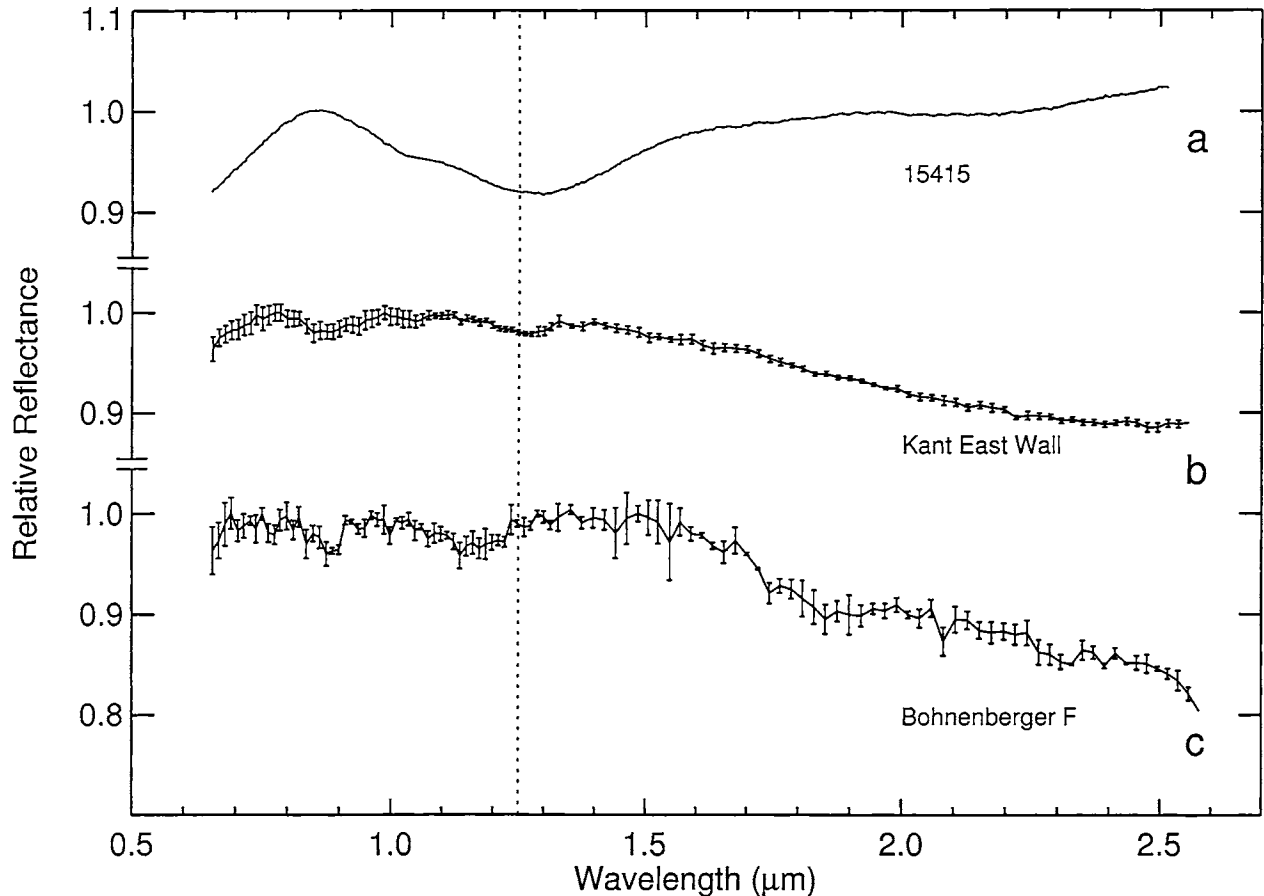


FIG. 8. (a) Continuum-removed version of a laboratory reflectance spectrum of Apollo 15 lunar sample 15415. The original absolute spectrum was retrieved from the web site of the RELAB spectral database at Brown University and is spectrum LS-JBA-122. The plagioclase iron impurity band centered near $1.25 \mu\text{m}$ is readily apparent. (b) and (c) Continuum-removed telescopic spectra of lunar pure anorthosites that may possess the $1.25 \mu\text{m}$ plagioclase absorption band. Spectrum (b) is for a portion of the eastern wall of Kant crater, collected from the area at $\sim 10.6^\circ \text{S}$, 20.1°E . Spectrum (c) is for Bohnenberger F, a 10 km in diameter crater located at $\sim 14.7^\circ \text{S}$, 39.6°E . These two spectra were collected with the Planetary Geosciences IRCVF spectrometer mounted on the University of Hawaii 2.2 m telescope on Mauna Kea (see Spudis *et al.*, 1989; Hawke *et al.*, 2002).

the lunar sample collection are rich resources for conducting spectral and compositional analog experiments. Important lessons applicable to all airless silicate bodies will no doubt be learned, even if the assumption of a pure anorthosite composition for Mercury eventually proves to be wrong. The match of featureless red spectra for the lunar pure anorthosites and Mercury is suggestive, but specific absorption features are needed to positively identify a mineral in reflectance spectra. The potential for spacecraft observation of diagnostic absorption features is the subject of the next section.

DIAGNOSTIC POTENTIAL OF SPACECRAFT SPECTRAL DATA FOR MERCURY

The preceding discussion demonstrates that at visible to near-infrared wavelengths, the reflectance spectra of lunar pure anorthosites and the planet Mercury are similar. They both lack strong absorption features and have comparable slopes. The mineral anorthite (plagioclase feldspar) can exhibit a

diagnostic absorption feature near $1.25 \mu\text{m}$ when trace amounts of ferrous iron (greater than $\sim 0.1 \text{ wt}\%$) are present in the structure as an impurity (Adams and Goulland, 1978), although the absorption band is lost if the material is shocked to high pressures (Adams *et al.*, 1979). This absorption is found in spectra of some lunar samples, as shown in Fig. 8a. The $1.25 \mu\text{m}$ plagioclase band has not been clearly identified in remote spectral measurements of lunar anorthosite, though it may be present in a spectrum of a portion of the east wall of Kant crater (Fig. 8b), and in a spectrum of Bohnenberger F crater (Fig. 8c) (Spudis *et al.*, 1989; Hawke *et al.*, 2002). The lack of an unambiguous $1.25 \mu\text{m}$ feature in spectra of lunar pure anorthosites has previously been attributed to the presence of shocked anorthosite (*e.g.*, Spudis *et al.*, 1984, 1989). This was considered a reasonable assumption because most known pure anorthosites are found in locations (such as crater central peaks or on basin rings) that conceivably experienced high levels of shock. However, recent spectral modeling by Lucey (2002) indicates that the effects of space weathering can obscure the plagioclase feature.

When spacecraft instruments make spectral measurements of Mercury at spatial resolutions greater than that available from Earth-based telescopes, it may be possible to observe the plagioclase iron impurity feature. The NASA MESSENGER mission to Mercury will carry a multispectral visible camera system and visible–infrared (0.3 to 1.4 μm) spectrograph (Gold *et al.*, 2001; McClintock and Holsclaw, 2001). The planned ESA Bepi Colombo orbiter payload includes a camera system for imaging in the range from 0.35 to 1.05 μm and an infrared spectrometer covering 0.8 to 2.8 μm (ESA, 2000). Discovery of a 1.25 μm feature would confirm the presence of pure anorthosite containing ferrous iron. Because of the influence of space weathering it is likely that only very freshly exposed surfaces would exhibit the band (Lucey, 2002), especially given the conditions for rapid regolith maturation at Mercury (Cintala, 1992). Therefore, optical maturity maps could be constructed from multispectral imaging of the mercurian surface, and used to rapidly identify particularly fresh craters. These could then be targeted for observation with instruments covering a wavelength range appropriate for measuring the plagioclase band. Shock erasure of the plagioclase feature is a complicating effect. Therefore smaller craters or portions of larger craters expected to have experienced lesser degrees of shock loading, such as wall slumps or near-rim ejecta, would be the best candidates for exhibiting the 1.25 μm band.

In addition to pure anorthosite, there are other possible mineralogies for Mercury that would have featureless reflectance spectra (*e.g.*, Lucey and Bell, 1989). Examples include quartz, magnesian pyroxene (enstatite or diopside), and magnesian olivine (forsterite). Burbine *et al.* (2002) investigated the spectral properties of aubrite meteorites (enstatite achondrites) and the minerals found in them. These rocks are highly reduced and the enstatite contains virtually no iron (Watters and Prinz, 1979). Burbine *et al.* (2002) concluded that a mercurian surface composed of enstatite basalt would have an absorption feature shortwards of $\sim 0.6 \mu\text{m}$ caused by sulfur or sulfides. Such a feature is not readily apparent in older Earth-based spectra of Mercury (*cf.*, Fig. 7), although the more recent spectra of Warell (2001; 2002, unpubl. data) hint at a broad shallow absorption shortwards of $0.6 \mu\text{m}$. Data collected by the future spacecraft missions should be able to delineate this absorption feature if it is indeed present. Burbine *et al.* (2002) note that the amounts of ferrous iron in aubrite material are below the levels believed to be required to bring about spectral reddening by SMFe produced during space weathering (Hapke, 1977, 2001a,b). However, as discussed by Noble and Pieters (2001), enough iron may be contributed by meteoritic sources to allow the reddening process to operate.

CONCLUSIONS

Areas of mature pure anorthosite have been identified on the Moon's farside using Clementine UV-vis FeO and optical maturity maps. They are found in regions of Imbrian- or

Nectarian-age plains or terra units. Clementine UV-vis spectra of the lunar mature pure anorthosites and Earth-based spectra for the planet Mercury both lack clear mineralogic absorption features and have similar spectral slopes. Lunar pure anorthosites, which by definition are composed of $>90\%$ plagioclase feldspar, are low in FeO content. Several lines of evidence also point to a mercurian surface dominated by material with very low FeO. Therefore, areas of lunar mature pure anorthosite can be studied as analogs for Mercury. The nature of the spectral slope beyond 0.75 μm may indicate that Mercury has even lower FeO than the lunar pure anorthosites.

Plagioclase can exhibit a diagnostic absorption band when trace amounts of ferrous iron are present in the crystal structure. This spectral feature is obscured by space weathering and shock. However, if the plagioclase band can be found in spectra of Mercury collected by future spacecraft, it will furnish a specific identification of rock and mineral types. We have described a search strategy targeted at fresh craters designed to maximize the chances of detecting the plagioclase band.

Mercury will provide a laboratory for the investigation of optical maturity and space weathering, especially in materials with low abundances of ferrous iron. Comparisons with the Moon will help to increase our knowledge of the processes by which crystalline rock becomes mature regolith.

Acknowledgments—This work was conducted with the help of the following grants from the NASA Planetary Geology & Geophysics program: NASW-02007 (D. T. B.), NAG5-8903 (B. R. H.), and NAG5-11516 (P. G. L.). The authors thank T. Burbine (National Museum of Natural History) and J. Warell (Uppsala University) for sharing their results ahead of publication. G. Smith (University of Hawaii) assisted with processing of some of the lunar telescopic spectra. This paper benefited greatly from reviews by J. Grier and F. Vilas. This is HIGP publication number 1222, and SOEST contribution 5995.

Editorial handling: B. E. Clark

REFERENCES

- ADAMS J. B. AND GOULLAND L. H. (1978) Plagioclase feldspars: Visible and near infrared diffuse reflectance spectra as applied to remote sensing. *Proc. Lunar Planet. Sci. Conf.* **9th**, 2901–2909.
- ADAMS J. B., HÖRZ F. AND GIBBONS R. V. (1979) Effects of shock-loading on the reflectance spectra of plagioclase, pyroxene, and glass. *Lunar Planet. Sci.* **10th**, 1–3.
- BLEWETT D. T., LUCEY P. G., HAWKE B. R. AND JOLLIFF B. L. (1997a) Clementine images of the lunar sample-return stations: Refinement of FeO and TiO₂ mapping techniques. *J. Geophys. Res.* **102**, 16 319–16 325.
- BLEWETT D. T., LUCEY P. G., HAWKE B. R., LING G. G. AND ROBINSON M. S. (1997b) A comparison of mercurian reflectance and spectral quantities with those of the Moon. *Icarus* **102**, 217–231.
- BURBINE T. H., MCCOY T. J., NITTLER L. R., BENEDIX G. K., CLOUTIS E. A. AND DICKINSON T. L. (2002) Spectra of extremely reduced assemblages: Implications for Mercury. *Meteorit. Planet. Sci.* **37**, 1233–1244.
- CINTALA M. J. (1992) Impact-induced thermal effects in the lunar and mercurian regoliths. *J. Geophys. Res.* **97**, 947–973.
- ELPHIC R. C., LAWRENCE D. J., FELDMAN W. C., BARRACLOUGH B. L., MAURICE S., BINDER A. B. AND LUCEY P. G. (1998) Lunar Fe

- and Ti abundances: Comparison of Lunar Prospector and Clementine data. *Science* **281**, 1493–1496.
- ELPHIC R. C., LAWRENCE D. J., FELDMAN W. C., BARRACLOUGH B. L., MAURICE S., BINDER A. B. AND LUCEY P. G. (2000) Lunar rare earth element distribution and ramifications for FeO and TiO₂: Lunar Prospector neutron spectrometer observations. *J. Geophys. Res.* **105**, 20 333–20 345.
- ELIASON E. M. *ET AL.* (1999) Digital processing for a global multispectral map of the Moon from the Clementine UVVIS imaging instrument (abstract). *Lunar Planet. Sci.* **30**, #1933, Lunar and Planetary Institute, Houston, Texas, USA (CD-ROM).
- EUROPEAN SPACE AGENCY (ESA) (2000) *Bepi-Colombo: Interdisciplinary Mission to Planet Mercury*. ESA BR-165, ESA Publications Division, Noordwijk, The Netherlands. 37 pp.
- GOLD R. E. *ET AL.* (2001) The MESSENGER scientific payload (abstract). In *Workshop on Mercury: Space Environment, Surface and Interior* (eds. M. Robinson and G. J. Taylor), pp. 29–30. LPI Contribution No. **1097**, Lunar and Planetary Institute, Houston, Texas, USA.
- GRIER J. A., MCEWEN A. S., LUCEY P. G., MILAZZO M. AND STROM R. G. (2001) Optical maturity of ejecta from large rayed lunar craters. *J. Geophys. Res.* **106**, 32 847–32 862.
- HAPKE B. (1977) Interpretations of optical observations of Mercury and the Moon. *Phys. Earth Planet. Int.* **15**, 264–274.
- HAPKE B. (1981) Bidirectional reflectance spectroscopy, 1. Theory. *J. Geophys. Res.* **86**, 3039–3054.
- HAPKE B. (1993) *Theory of Reflectance and Emittance Spectroscopy*. Cambridge University Press, Cambridge, U.K. 455 pp.
- HAPKE B. (2001a) Space weathering from Mercury to the asteroid belt. *J. Geophys. Res.* **106**, 10 039–10 073.
- HAPKE B. (2001b) Space weathering and the composition of the crust of Mercury (abstract). In *Workshop on Mercury: Space Environment, Surface and Interior* (eds. M. Robinson and G. J. Taylor), p. 35. LPI Contribution No. **1097**, Lunar and Planetary Institute, Houston, Texas, USA.
- HAWKE B. R., LUCEY P. G., TAYLOR G. J., SPUDIS P. D., BELL J. F., PETERSON C. A., BLEWETT D. AND HORTON K. (1991) Remote sensing studies of the Orientale region of the Moon: A pre-Galileo view. *Geophys. Res. Lett.* **18**, 2141–2144.
- HAWKE B. R., PETERSON C. A., LUCEY P. G., TAYLOR G. J., BLEWETT D. T., CAMPBELL B. A., COOMBS C. R. AND SPUDIS P. D. (1993a) Remote sensing studies of the terrain northwest of Humorum basin. *Geophys. Res. Lett.* **20**, 419–422.
- HAWKE B. R., SPUDIS P. D., TAYLOR G. J., LUCEY P. G. AND PETERSON C. A. (1993b) The distribution and modes of occurrence of anorthosite on the Moon (abstract). *Meteoritics* **28**, 361.
- HAWKE B. R., PETERSON C. A., BLEWETT D. T., BUSSEY D. B. J., LUCEY P. G., TAYLOR G. J. AND SPUDIS P. D. (2002) The distribution and modes of occurrence of lunar anorthosite. *J. Geophys. Res., Planets* (in press).
- ISBELL C. E. *ET AL.* (1999) Clementine: A multispectral digital image model archive of the Moon (abstract). *Lunar Planet. Sci.* **30**, #1812, Lunar and Planetary Institute, Houston, Texas, USA (CD-ROM).
- JEANLOZ R., MITCHELL D. L., SPRAGUE A. L. AND DE PATER I. (1995) Evidence for a basalt-free surface on Mercury and implications for internal heat. *Science* **268**, 1455–1457.
- LAWRENCE D. J., FELDMAN W. C., ELPHIC R., LITTLE R., PRETTYMAN T. H., MAURICE S., LUCEY P. G. AND BINDER A. B. (2002) Iron abundances on the lunar surface as measured by the Lunar Prospector gamma-ray and neutron spectrometers. *J. Geophys. Res., Planets* (in press).
- LUCEY P. G. (2002) Radiative transfer model constraints on the shock state of remotely sensed lunar anorthosites. *Geophys. Res. Lett.* **29**, no. 10, 10.1029/2001GL014655, 31 May 2002.
- LUCEY P. G. AND BELL J. F. (1989) An enstatite crustal composition for Mercury? (abstract). *Lunar Planet. Sci.* **20**, 592–593.
- LUCEY P. G., TAYLOR G. J. AND MALARET E. (1995) Abundance and distribution of iron on the Moon. *Science* **268**, 1150–1153.
- LUCEY P. G., BLEWETT D. T. AND HAWKE B. R. (1998) Mapping the FeO and TiO₂ content of the lunar surface with multispectral imagery. *J. Geophys. Res.* **103**, 3679–3699.
- LUCEY P. G., BLEWETT D. T. AND JOLLIFF B. L. (2000a) Lunar iron and titanium abundance algorithms based on final processing of Clementine UVVIS data. *J. Geophys. Res.* **105**, 20 297–20 305.
- LUCEY P. G., BLEWETT D. T., TAYLOR G. J. AND HAWKE B. R. (2000b) Imaging of lunar surface maturity. *J. Geophys. Res.* **105**, 20 377–20 386.
- MCCLINTOCK W. M. AND HOLSCLAW G. M. (2001) The Mercury atmospheric and surface composition spectrometer (MASCs) for the MESSENGER mission (abstract). In *Workshop on Mercury: Space Environment, Surface and Interior* (eds. M. Robinson and G. J. Taylor), p. 62. LPI Contribution No. **1097**, Lunar and Planetary Institute, Houston, Texas, USA.
- MCCORD T. B. AND CLARK R. N. (1979) The Mercury soil: Presence of Fe²⁺. *J. Geophys. Res.* **84**, 7664–7668.
- NOBLE S. K. AND PIETERS C. M. (2001) Space weathering in the mercurian environment (abstract). In *Workshop on Mercury: Space Environment, Surface and Interior* (eds. M. Robinson and G. J. Taylor), pp. 68–69. LPI Contribution No. **1097**, Lunar and Planetary Institute, Houston, Texas, USA.
- NOZETTE S. *ET AL.* (1994) The Clementine mission to the Moon: Scientific overview. *Science* **266**, 1835–1839.
- PETERSON C. A., HAWKE B. R., LUCEY P. G., TAYLOR G. J., BLEWETT D. T. AND SPUDIS P. D. (2001) Lunar anorthosite: A global layer (abstract). *Lunar Planet. Sci.* **32**, #1592, Lunar and Planetary Institute, Houston, Texas, USA (CD-ROM).
- PIETERS C. M. (1986) Composition of the lunar highland crust from near-infrared spectroscopy. *Rev. Geophys.* **24**, 557–578.
- PIETERS C. M. (1993) Compositional diversity and stratigraphy of the lunar crust derived from reflectance spectroscopy. In *Remote Geochemical Analysis* (eds. C. M. Pieters and P. A. J. Englert), pp. 309–339. Cambridge Univ. Press, Cambridge, U.K.
- PIETERS C. M., TAYLOR L. A., NOBLE S. K., KELLER L. P., HAPKE B., MORRIS R. V., ALLEN C. C., MCKAY D. S. AND WENTWORTH S. (2000) Space weathering on airless bodies: Resolving a mystery with lunar samples. *Meteorit. Planet. Sci.* **35**, 1101–1107.
- ROBINSON M. S. AND MCEWEN A. S. (1997) Mapping of the Moon by Clementine. *Adv. Space Res.* **19**, 1523–1533.
- ROBINSON M. S., MCEWEN A. S., ELIASON E., LEE E. M., MALARET E. AND LUCEY P. G. (1999) Clementine UVVIS global mosaic: A new tool for understanding the lunar crust (abstract). *Lunar Planet. Sci.* **30**, #1931, Lunar and Planetary Institute, Houston, Texas, USA (CD-ROM).
- SCOTT D. H., MCCAULEY J. F. AND WEST M. N. (1977) *Geologic Map of the West Side of the Moon*. U. S. Geol. Survey Misc. Investigation Map I-1034, Reston, Virginia, USA.
- SPRAGUE A. L., KOZLOWSKI R. W. H., WITTEBORN F. C., CRIUKSHANK D. P. AND WOODEN D. H. (1994) Mercury: Evidence for anorthosite and basalt from mid-infrared (7.3–13.5 μm) spectroscopy. *Icarus* **109**, 156–167.
- SPUDIS P. D., HAWKE B. R. AND LUCEY P. G. (1984) Composition of Orientale basin deposits and implications for the lunar basin-forming process. *Proc. Lunar Planet. Sci. Conf. 15th, J. Geophys. Res.* **89** (Suppl.), C197–C210.
- SPUDIS P. D., HAWKE B. R. AND LUCEY P. G. (1989) Geology and deposits of the lunar Nectaris basin. *Proc. Lunar Planet. Sci. Conf. 19th*, 51–60.

- STÖFFLER D., KNOLL H-D., MARVIN U. B., SIMONDS C. H. AND WARREN P. W. (1980) Recommended classification and nomenclature of lunar highland rocks—A committee report. In *Proceedings of the Conference on the Lunar Highlands Crust* (eds. J. J. Papike and R. B. Merrill), pp. 51–70. Pergamon Press, New York, New York, USA.
- STUART-ALEXANDER D. E. (1978) *Geologic Map of the Central Far Side of the Moon*. U. S. Geol. Survey Misc. Investigation Map I-1047, Reston, Virginia, USA.
- TOMPKINS S. AND PIETERS C. M. (1999) Mineralogy of the lunar crust: Results from Clementine. *Meteorit. Planet. Sci.* **34**, 25–41.
- VILAS F. (1985) Mercury: Absence of crystalline Fe in the regolith. *Icarus* **64**, 133–138.
- VILAS F. (1988) Surface composition of Mercury from reflectance spectrophotometry. In *Mercury* (eds. F. Vilas, C. R. Chapman and M. S. Matthews), pp. 59–76. Univ. Arizona Press, Tucson, Arizona, USA.
- WARELL J. (2001) Disk-resolved multicolor photometry and spectroscopy of Mercury (abstract). In *Workshop on Mercury: Space Environment, Surface and Interior* (eds. M. Robinson and G. J. Taylor), p. 108. LPI Contribution No. **1097**, Lunar and Planetary Institute, Houston, Texas, USA.
- WATTERS T. R. AND PRINZ M. (1979) Aubrites: Their origin and relationship to enstatite chondrites. *Proc. Lunar Planet. Sci. Conf.* **10th**, 1073–1093.
-